NANO LETTERS

2006
Vol. 6, No. 5
963−968

Variable Pressure Electron Beam Lithography (VP-*e*BL): A New Tool for Direct Patterning of Nanometer-Scale Features on Substrates with Low Electrical Conductivity

Benjamin D. Myers and Vinayak P. Dravid*

Department of Materials Science and Engineering and NUANCE Center, Northwestern University, 2220 Campus Drive, Evanston, Illinois 60208

Received January 19, 2006; Revised Manuscript Received March 14, 2006

ABSTRACT

We introduce variable pressure electron beam lithography (VP-*e*BL), as a new approach for the fabrication of nanometer-scale structures on electrically insulating substrates. This novel approach combines the high-resolution patterning capability of electron beam lithography with the charge-balance mechanism of the variable pressure scanning electron microscope (VPSEM) to control charging effects during pattern exposure. VP-*e*BL eliminates the need for any of the additional materials or processing steps required to eliminate pattern distortion artifacts during high vacuum *e*BL patterning on such substrates. Preliminary characterization of the VP-*e*BL process is presented, which demonstrates no significant change in ultimate pattern definition or enhancement of the local proximity effects due to primary beam scattering. In addition, we find that the shape of the scattering profile in the resist layer is modified in the presence of the chamber gas, allowing improved pattern definition at higher pressures.

The development of tools and processes for fabrication of structures with dimensions less than 100 nanometers is critical for the implementation of practical nanoscale devices and the study of the unique phenomena at this length scale. Electron beam lithography (*e*BL) using organic thin film resists is among the most promising and widely applied techniques, owing largely to its capability for high-resolution patterning.[1] For a typical high resolution *e*BL process, the resist layer (usually an electron sensitive polymer film) is less than 300 nm thick in order to optimize the exposure profile in the resist. Given the thin resist layer and the high beam energies typically employed (30−100 kV), the vast majority of the electron dose is deposited in the substrate. Patterning on grounded and/or conductive substrates is straightforward, but using *e*BL to pattern on electrically insulating substrates often results in the formation of strong electrostatic fields at the sample surface in the absence of a means for charge dissipation. The resulting fields can be strong enough to deflect the incident electron beam or cause severe astigmatism, resulting in pattern distortion.[2] In addition, the use of conductive substrates does not necessarily eliminate charging problems, especially with the case of thicker resists or low-energy *e*BL.[3,4]

Electrically insulating substrates are required for a number of different applications in both existing and emerging technologies. These include conventional materials in semiconductor processing such as SiO_2 and Si_3N_4, materials for optoelectronics such as GaN, sapphire, and glass as well as polymers for applications including so-called flexible plastic electronics. Several methods have been developed to allow *e*BL patterning on insulators without charging-induced pattern distortion. The most common method involves sputter coating or evaporating a thin metal film (typically ∼10 nm) on the surface of the resist layer, which is grounded during the exposure process.[5] This method is effective in minimizing pattern distortion although additional process steps are required for film deposition prior to exposure and for film removal prior to development. The film removal process, typically a wet etch, also raises concerns regarding chemical compatibility with the resist or substrate materials. Other proposed methods include using an ion shower method and the use of conductive polymer resists.[6,7] However, there is currently no widely applicable method for eliminating substrate charging effects without additional processing steps or the use of nonstandard materials. In the present work, we describe an effective method for in situ charge dissipation that is compatible with virtually any substrate and resist system.

* Corresponding author. E-mail: v-dravid@northwestern.edu.

10.1021/nl0601278 CCC: $33.50
Published on Web 04/04/2006

Variable pressure scanning electron microscopy (VPSEM) allows for the imaging of electrically insulating materials in pristine condition, without the need for conductive coatings or lengthy and difficult dehydration processes.[8] This is accomplished by the introduction of a low pressure of gas (typically water vapor, N_2, Ar, or He) into the SEM chamber and the use differential pumping to maintain high vacuum in the electron column. The presence of the gas in the chamber has several important consequences. First, the gas molecules may be ionized by electron impact and these positive gas ions may migrate to the negatively charged surface and balance the surface charge. The exact mechanism by which this charge-balance occurs is not fully understood, but it likely involves a combination of electron−ion recombination and space charge effects.[9] Second, the chamber gas serves to amplify the secondary electron (SE) signal by the so-called "gas cascade" effect.[10] Third, the primary electron beam will be scattered to some extent by collisions with the gas molecules resulting in the formation of a beam "skirt" around the focused primary beam at the sample surface. The number of primary electrons scattered and their distribution in the skirt depends on the energy of the primary electrons, gas type, gas pressure, and beam−gas path length (BGPL).[8] It should be emphasized that even though charging is controlled sufficiently in the VPSEM to allow artifact-free SE imaging, significant time-dependent electrostatic potentials still exist both below the sample surface and in the chamber above the sample.[11]

Previous work has demonstrated the use of a VPSEM in a recurrent *e*BL process for the generation of 3D structures utilizing a low-energy primary beam and multiple exposure/develop cycles.[12,13] For the low beam energy (5 keV) and resist thickness used, the electron beam interaction is completely confined to the electrically insulating resist layer, resulting in charging effects that were controlled with the introduction of water vapor to the chamber. In addition to demonstrating the capability of the recurrent *e*BL technique, an increase in pattern line width with increasing gas pressure was shown as a primary result. However, this work did not address the issue of patterning features smaller than 100 nm. In the present work, we demonstrate the VP-*e*BL technique for the fabrication of truly nanometer-scale structures on technologically important insulating substrates. In addition to demonstrating proof of concept, we also present results from preliminary characterization of the VP-*e*BL process to investigate the effects of important parameters, including beam energy, gas pressure, and pattern density. It is argued that VP-*e*BL is an effective approach to enable patterning of functional nanostructures and device geometries for arbitrary substrates, especially insulating ones such as ceramics and polymers, which are critical in the technological development of emerging nanoscale devices and components. Thus, we believe that VP-*e*BL ushers a new era in site- and shape-specific patterning of functional nanostructures on technologically important substrate systems.

Borosilicate glass cover slips and lightly doped (>8 ohms-cm) n-type (100) oriented silicon were used as substrates for these experiments. The substrates were prepared by spin coating 950 kg/mol PMMA electron-sensitive resist from Microchem, Inc. to produce a uniform resist layer. Experiments involving pattern generation though liftoff processing were carried out using 3% PMMA solids in anisole with a 4000 rpm spin speed to achieve ~150 nm resist thickness. Cross-section studies were carried out with 9% solids PMMA in anisole with a 2000 rpm spin speed to achieve a resist thickness of approximately 1 μm on the silicon substrates. After spin coating, the samples were placed on a hot plate at 180 °C for 90 s in order to soft-bake the resist layer. PMMA coated glass substrates were hard-masked with a clean glass slide and half the sample was sputter coated with a 15−20 nm film of Au/Pd. This coated region was grounded during exposure, allowing for charge dissipation during final focusing prior to patterning on the adjacent, uncoated region.

Electron beam exposure was carried out with a field emission gun equipped Quanta 600F ESEM from FEI Corporation integrated with an NPGS lithography system from JC Nabity, Inc. Water vapor was used as the chamber gas, and an additional pressure-limiting aperture cone (3 mm) was installed for all experiments. The system was configured using the large field (off-axis) gaseous secondary electron detector (LFSED) for variable pressure experiments, and the Everhart−Thornley detector was used for high vacuum experiments. The spot size was adjusted to carry out all exposures with a constant beam current of approximately 28 pA (±1.5 pA). Patterns were developed in a 3:1 2-propanol/methyl isobutyl ketone solution for 75 s, followed by rinsing in 2-propanol for 45 s. To transfer patterns to the substrate, samples were sputter coated with 15 nm of Au/Pd and then lift-off was performed in acetone with ultrasonic agitation followed by rinsing in 2-propanol. The resulting patterns were imaged in the Quanta ESEM in low vacuum mode with the backscattered electron detector or LFSED. Cross-sectional samples were prepared by cleaving in liquid nitrogen after developing and then sputter coated with 5 nm of Au/Pd and imaged with a LEO Gemini 1525 high-resolution SEM.

The first experiments were designed to determine whether the charge-balance mechanism present in the VPSEM is capable of reducing or eliminating pattern distortion. For this proof of concept, we exposed a number of arbitrary pattern designs on glass substrates under high vacuum conditions and under different chamber pressures. A qualitative assessment of the patterns determined a threshold for pattern distortion with a chamber pressure near 0.6−0.7 Torr for a 7 mm working distance (~4 mm BGPL), 30 keV beam energy, and the minimum dwell time required to completely expose the resist. The absolute value of this threshold will depend on many factors including substrate/resist composition, exposure conditions, and pattern geometry but corresponds quite well with experimental evidence for minimum pressures to achieve charge balance during imaging (0.1−0.6 Torr).[14] A comparison of exposures under high vacuum conditions and with 0.4 and 1 Torr chamber pressure is shown in Figure 1, which illustrates the effectiveness of the VP-*e*BL technique for minimizing pattern distortion on insulating substrates.

Figure 1. VPSEM images of 15 nm Au/Pd film patterned on a glass substrate with a 30 keV primary beam energy under (a) high vacuum, (b) 0.4 Torr, and (c) 1 Torr. The dashed red line indicates the pattern dimensions as written. The letters N, U, N, C, and E were patterned in order, followed by A in order to highlight the charging-induced pattern displacement. The pattern exposed using the VP-*e*BL process with 1 Torr chamber pressure shows no significant distortion or displacement.

To further characterize the process, we investigated the effects of primary beam scattering (i.e., beam skirting) on ultimate pattern definition and pattern density. To study these effects, cross-sectional samples were exposed with different primary beam energies and chamber pressures. Figure 2 shows cross sections of a line array patterned with a relatively low energy beam (5 keV) on the same substrate under identical conditions, with the exception of chamber pressure. Exposures were carried out in high vacuum, as well as 0.25, 0.5, and 1 Torr with a uniform line dose of 0.5 nC. There is a significant change in the size of the developed trench with increasing gas pressure. The volume of material removed during developing is a function of the distribution of energy deposited into the resist, above some critical threshold. Therefore, we attribute the reduction in trench size primarily to the delocalization of some primary electrons resulting in an effective attenuation of the beam current. However, it is possible that the effect is really a convolution of beam skirting effects and space charge effects. In addition, there is no significant change in the width of the trench at the resist surface, suggesting that the diameter of the primary electron beam is not altered significantly.

Space charge effects can be seen by analyzing cross sections exposed with higher beam energies, where the skirting effect is minimized. Samples for cross-sectional analysis were exposed with a 30 keV primary beam, using a constant electron dose of 2 nC/cm under high vacuum conditions and at pressures of 1 and 2 Torr as shown in Figure 3. A comparison of these cross sections indicates a very small change in the trench depth with increasing chamber pressure. This is reasonable because scattering of the primary beam will be significantly less probable with increasing energy, hence decreasing the scattering cross

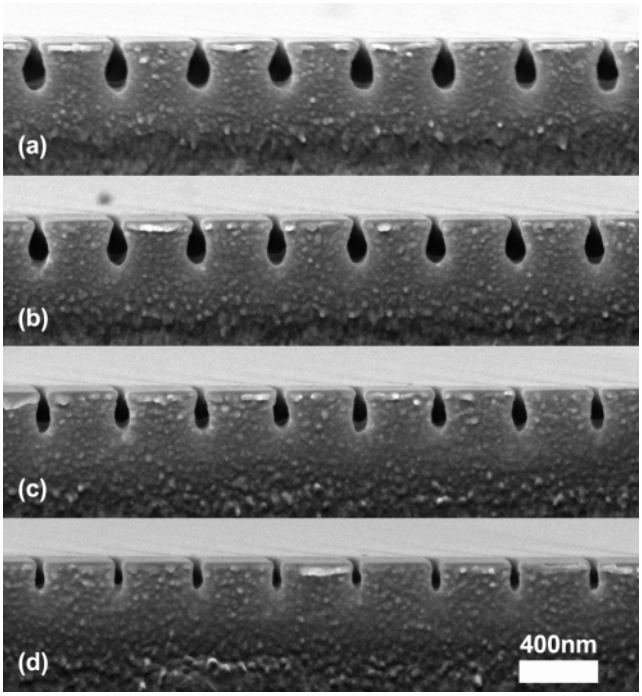

Figure 2. SEM images of PMMA cross sections following exposure of line arrays with a 5 keV primary beam energy and uniform line dose of 0.5 nC/cm under (a) high vacuum, (b) 0.25 Torr, (c) 0.5 Torr, and (d) 1 Torr. The trench size decreases with increasing gas pressure as a result of primary beam scattering and the subsequent delocalization of a large number of primary electrons.

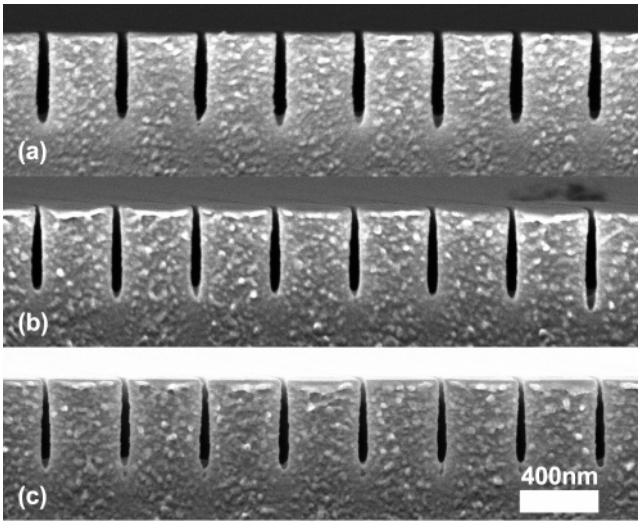

Figure 3. SEM images of PMMA cross sections following exposure of line arrays with a 30 keV primary beam energy and uniform line dose of 2 nC/cm under (a) high vacuum, (b) 1 Torr, and (c) 2 Torr. There is only a slight change in trench depth, but the shape of the trench is significantly altered, likely due to modification of the subsurface space charge by the action positive gas ions in the chamber.

section. A closer examination of the trench shape indicates that the high vacuum exposures have a much more uniform profile throughout the depth, whereas exposures at 1 and 2 Torr have increasingly "teardrop"-shaped trenches, narrower at the top, becoming wider with increasing depth. Although the silicon substrate is relatively conductive, the thick resist

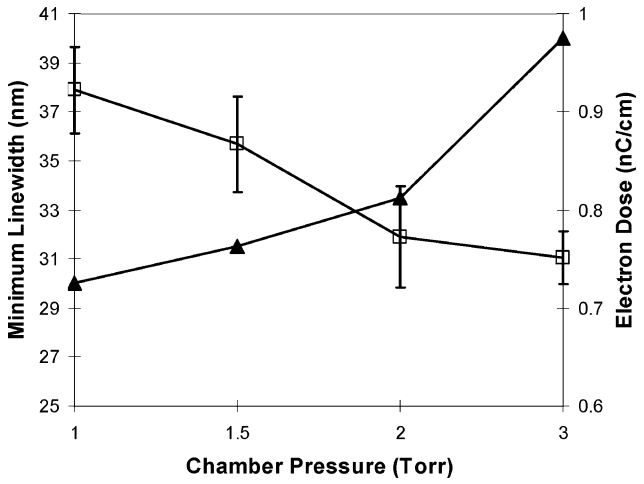

Figure 4. Minimum pattern line width (□) and electron dose (▲) for 15 keV exposures as a function of chamber pressure. The electron dose required for complete exposure increases with pressure due to beam skirting, and the line width decreases presumably due to a modification of the subsurface space charge distribution.

layer may prevent complete charge dissipation, and this effect can likely be attributed to charging in the resist layer. This mechanism is supported by Monte Carlo simulations, which show a change in the shape of the electron beam interaction as a function of precharge.[15] More recent simulations have investigated the dynamic evolution of the charge distribution.[16] However, the charging process with VP-*e*BL is not only dynamic but likely depends on gas scattering and ionization, pattern geometry, writing order, and other factors.

A similar effect can be seen in patterns exposed on glass substrates with increasing gas pressure. Because the effective probe current decreases with increasing primary beam scattering as shown above, constant dose studies cannot be used to assess minimum feature sizes. Instead, patterns were exposed using an array of doses (25 pC/cm steps) and then processed with identical developing and liftoff conditions. The features patterned were circular single-pass lines with 5 μm diameter; this shape was chosen for facile assessment of any astigmatism, which could otherwise impact line-width measurements. In addition, the spacing between features was also 5 μm to minimize any proximity effects. An intermediate primary beam energy of 15 keV was used for these experiments in order to achieve larger minimum feature sizes, which allows for better measurement statistics (imaging resolution is limited to $\sim$3 nm) and because the lower beam energy will result in an enhanced skirting effect. The resulting patterns were then analyzed, and the line width was measured for the lowest dose exposure resulting in complete transfer to the substrate. The results in Figure 4 show that the minimum pattern line width decreases with increasing gas pressure, whereas the dose required for complete exposure increases due to skirting effects.

We attribute the line-width variation to a modification of the subsurface space charge distribution by the presence of water vapor and its influence on the scattering and charging processes and note a similar trend with increased BGPL. There has been some evidence of an electron-beam-induced etching process in the presence of water vapor, which could lead to a similar result because the resist layer would be locally thinned during exposure.[17,18] However, we investigated the possibility of electron-beam-induced etching during the exposure process in the presence of water vapor, inert gas (Ar), and under high vacuum conditions. AFM analysis of the exposed resist (prior to developing) showed no significant difference in resist thickness change for the different chamber conditions. This indicates that in situ etching of the resist is not a significant factor for the VP-*e*BL process, likely due to the use of electron doses several orders of magnitude lower than those in the cited references. In addition, even on the significantly more conductive silicon substrates, a similar trend of improved pattern definition with increasing gas pressure is seen. In fact, using the VP-*e*BL process allows for the generation of *smaller* features than with standard high vacuum processing for these semiconducting substrates.

However, we find that this apparently simple relationship is complicated when pattern features are brought in close proximity. Arrays of lines with different pitches were exposed on PMMA coated glass and silicon with variations in the chamber pressure. For these 15 keV exposures, the minimum pitch that could be achieved was about 100 nm. Although a relationship between gas pressure and pattern dimensions is not clear, these patterns can be analyzed to assess the effects of primary electron scattering on proximity effects. A proximity dose effect in traditional, high vacuum *e*BL is the result of backscattered electrons or so-called fast secondary electrons with a range far exceeding that of secondary electrons generated during forward scattering. These scattered electrons can contribute a background dose to neighboring features and are typically compensated for with dose modulation. It is an important factor to consider whether the beam skirt contributes to any additional proximity effect. This was investigated by first applying the same dose array method (25 pC/cm steps) to find the minimum dose required to expose the line arrays for each set of conditions. The widths of the lines in the array were then measured as a function of their distance from the edge of the array.

Measurements of line widths for the 100 nm pitch line arrays on both glass and silicon substrates are shown in Figure 5. These data show a significant change in pattern line width as a function of position from the edge of the array, independent of substrate type or gas pressure. The effect of this proximity dose appears to saturate at a distance of about 1 μm from the first line in the array. As the pitch of the line arrays is increased to more than 200 nm, the proximity effect becomes negligible and the minimum line width approaches that of isolated features. When compared to high vacuum exposures on silicon, the VP-*e*BL process showed somewhat lower average line widths, possibly because of charging effects in the lightly doped silicon even though no significant pattern distortion was noted under these conditions.

These results indicate that although a portion of the primary electron beam is scattered, these scattered electrons

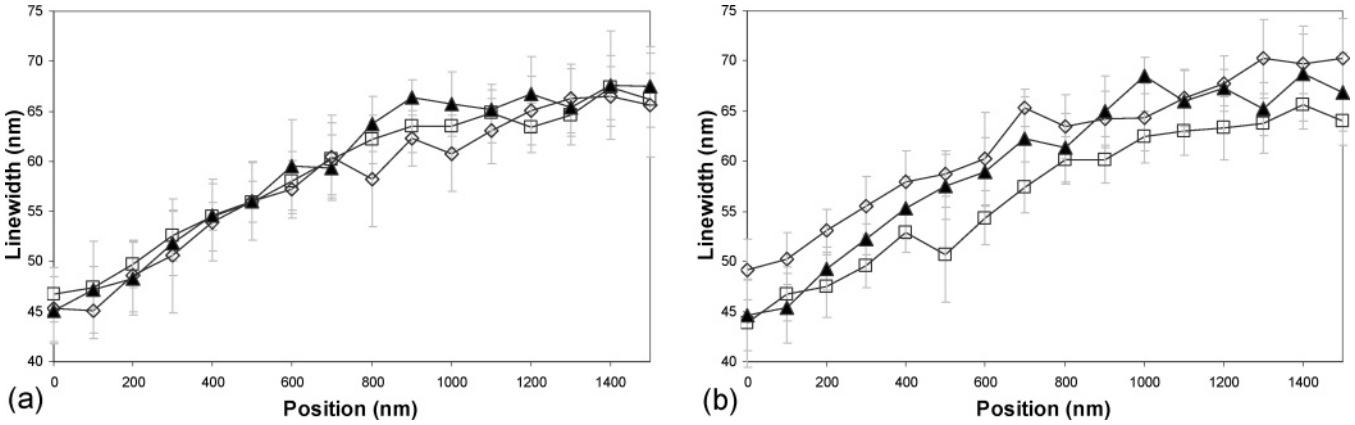

Figure 5. Pattern line widths as a function of position from the edge of line arrays with 100 nm pitch for (a) glass and (b) silicon substrates. The electron dose varied for each pattern due to loss of current to beam skirt; glass: 0.5 Torr (◊) − 0.575 nC/cm, 1 Torr (□) − 0.650 nC/cm, 2 Torr (▲) − 0.700 nC/cm; silicon: high vacuum (◊) − 0.625 nC/cm, 1 Torr (□) − 0.650 nC/cm, 2 Torr (▲) − 0.725 nC/cm. These data show no enhancement in the local proximity effect with increasing gas pressure.

do not contribute to any additional local proximity effect. It may be that the distribution of scattered electrons in the skirt is broad in comparison to the patterned region in this study. A relatively broad distribution of electrons in the skirt would result in a minimal change in the resulting width of the primary beam after scattering. This is corroborated by measurements of imaging resolution in the VPSEM, which indicate a relatively small change in image resolution with increasing gas pressure.[11] However, although there is some information in the literature describing beam skirting out to several hundred micrometers, there is currently no experimental data for the distribution within ~1 micrometer of the primary beam.[19−21] Although the beam skirt does not appear to contribute significantly to short-range proximity effects, the patterned area in this study was relatively small ($100 \times 100\ \mu m^2$) and there may be long-range proximity effects that impact large-area patterns.

Finally, we explored the resolution limits of the VP-*e*BL technique on our system to determine the minimum feature sizes possible on glass substrates in comparison to high vacuum processing on conductive substrates (~15−20 nm). For this test, arrays of 200 nm pitch, single-pass lines with intentional gaps were patterned with a 30 keV primary beam energy and 2 Torr chamber pressure. The same 25 pC/cm dose step method was employed, and the results shown in Figure 6 indicate that employing the VP-*e*BL process with an electrically insulating substrate can achieve feature sizes comparable to a high vacuum *e*BL process free of specimen charging.

In conclusion, we have demonstrated a new method for charge dissipation during *e*BL patterning on electrically insulating substrates. The VP-*e*BL technique allows the use of any substrate/resist system and eliminates additional process steps required for deposition and removal of a conductive top coat. We have shown that the VP-*e*BL process eliminates charging-induced pattern distortion for chamber pressures in excess of 1 Torr of water vapor. We also find that the VP-*e*BL process may allow for patterning of finer features on semiconducting substrates in comparison to high vacuum processing. The scattering of the electron beam by

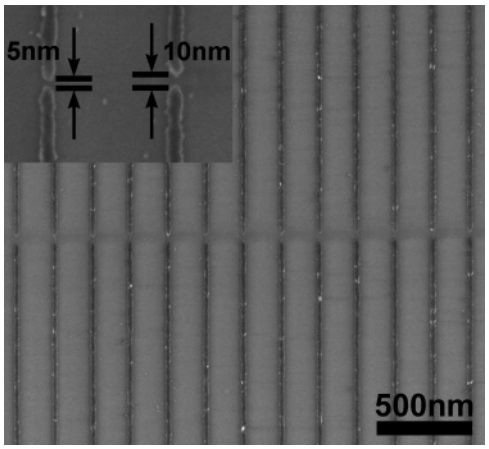

Figure 6. VPSEM images of Au/Pd patterns on glass substrates demonstrating the high resolution and high pattern density capabilities of the VP-*e*BL process, showing ~20 nm lines with 200 nm pitch and intentional gaps of ~5 and 10 nm (inset).

the chamber gas has no significant impact on the ultimate pattern resolution and we are able to achieve line widths comparable to those achieved with high vacuum exposure on conductive substrates (<20 nm). Analysis of cross-sectional samples indicates a significant amount of primary beam scattering for low beam energy (5 keV). At higher beam energy (30 keV), the scattering profile in the resist indicates a modification of the subsurface space charge distribution and results in more teardrop-shaped profiles with higher chamber pressure. Characterization of the process demonstrates no enhancement of local proximity effects due to scattering of the primary beam for 15 keV exposures. For isolated features, we have observed a decrease in the minimum feature size with increasing gas pressure and BGPL, which is attributed to the modified space charge distribution. The exact mechanism and details of this relationship are still under investigation and we are currently running additional experiments and simulations to explain this phenomenon.

Acknowledgment. This work is partially supported by the Nanoscale Science and Engineering Initiative of the

National Science Foundation under NSF Award No. EEC-0118025 and the NU*ANCE* Center staff development program. We thank Dr. Brad Thiel (SUNY Albany) for valuable discussions. All patterning and imaging was carried out in the EPIC facilities in the NU*ANCE* Center at Northwestern University. NU*ANCE* Center is supported by NSF-NSEC, NSF-MRSEC, Keck Foundation, the State of Illinois, and Northwestern University.

References

(1) Rai-Choudhury, P. *Handbook of Microlithography, Micromachining, and Microfabrication*; SPIE Optical Engineering Press: Bellingham, WA, 1997; Vol. 1: Microlithography.
(2) Cummings, K. D.; Kiersh, M. *J. Vac. Sci. Technol., B* **1989**, *7*, 1536−1539.
(3) Liu, W.; Ingino, J.; Pease, R. F. *J. Vac. Sci. Technol., B* **1995**, *13*, 1979−1983.
(4) Mun, L. M.; Drouin, D.; Lavallee, E.; Beauvais, J. *Microsc. Microanal.* **2004**, *10*, 804−809.
(5) Cumming, D. R. S.; Khandaker, I. I.; Thoms, S.; Casey, B. G. *J. Vac. Sci. Technol., B* **1997**, *15*, 2859−2863.
(6) Angelopoulos, M.; Patel, N.; Shaw, J. M.; Labianca, N. C.; Rishton, S. A. *J. Vac. Sci. Technol., B* **1993**, *11*, 2794−2797.
(7) Sakashita, T.; Nomura, N.; Hashimoto, K.; Koizumi, T.; Harafuji, K.; Misaka, A.; Sawada, N.; Kawakita, K. *J. Vac. Sci. Technol., B* **1989**, *7*, 1528−1531.
(8) Danilatos, G. D. *Adv. Electron. Electron Phys.* **1988**, *71*, 109−250.
(9) Cazaux, J. *Microsc. Microanal.* **2004**, *10*, 670−684.
(10) Thiel, B. L.; Bache, I. C.; Fletcher, A. L.; Meredith, P.; Donald, A. M. *J. Microsc. (Oxford, U.K.)* **1997**, *187*, 143−157.
(11) Thiel, B. L.; Toth, M. *J. Appl. Phys.* **2005**, *97*.
(12) Paul, B. K. *Scanning* **1997**, *19*, 466−468.
(13) Paul, B. K.; Klimkiewicz, M. *Scanning* **1996**, *18*, 490−496.
(14) Meredith, P.; Donald, A. M.; Thiel, B. *Scanning* **1996**, *18*, 467−473.
(15) Kotera, M.; Suga, H. *J. Appl. Phys.* **1988**, *63*, 261−268.
(16) Renoud, R.; Mady, F.; Ganachaud, J. P. *J. Phys.: Condens. Matter* **2002**, *14*, 231−247.
(17) Yuzvinsky, T. D.; Fennimore, A. M.; Mickelson, W.; Esquivias, C.; Zettl, A. *Appl. Phys. Lett.* **2005**, *86*.
(18) Kohlmann-von Platen, K. T.; Bruenger, W. H. *J. Vac. Sci. Technol., B* **1996**, *14*, 4262−4266.
(19) Belkorissat, R.; Kadoun, A. E. D.; Dupeyrat, M.; Khelifa, B.; Mathieu, C. *Microchim. Acta* **2004**, *147*, 135−139.
(20) Kadoun, A.; Belkorissat, R.; Mathieu, C.; Khelifa, B. *J. Trace Microprobe Tech.* **2003**, *21*, 229−238.
(21) Wight, S.; Gillen, G.; Herne, T. *Scanning* **1997**, *19*, 71−74.

NL0601278